IEEE Access
Multidisciplinary | Rapid Review | Open Access Journal

Received 20 August 2022, accepted 26 September 2022, date of publication 3 October 2022, date of current version 11 October 2022.

Digital Object Identifier 10.1109/ACCESS.2022.3211649

APPLIED RESEARCH

Deep-Sea Membrane Condition Monitoring Based on Wireless Humidity Measurement

XIAOYONG NI[1], XUHUA CHEN[1], YEDAN ZHANG[1], WANJUN LU[2], HONGJIAN ZHANG[3], LIFU ZHANG[2], AND XIAOYU XIONG[1]

[1]Department of Mechanical Engineering and Electronic Information, China University of Geosciences, Wuhan, Hubei 430074, China
[2]Department of Marine Science and Technology, China University of Geosciences, Wuhan, Hubei 430074, China
[3]Institute of Electronic Information, Wuhan Qingchuan University, Wuhan, Hubei 430204, China

Corresponding author: Hongjian Zhang (wh_zhanghj@163.com)

This work was supported in part by the National Key Research and Development Program of China under Grant 2018YFC0310006-04, and in part by the National Science Foundation of China under Grant 92058208.

ABSTRACT Membrane-based separation technology is widely used to analyze the chemical and isotopic composition of the dissolved gases in marine environments. Monitoring the membrane working condition and effectiveness of underwater spectrometer is a necessary and challenging task. In order to achieve this goal, a wireless humidity measurement method using low-frequency signal through metal plates is proposed. The humidity measurement consists of a transmitter and a receiver. The transmitter is enclosed by 5 mm-thick stainless steel plates to meet the safety requirements. The capacitance of the humidity sensor is modulated into the frequency of transmission signal with an *LC*-type oscillator and the working frequency is about 10 kHz. The frequency of received signal relates to many parameters, such as transmitter movement distance, plate material and thickness, which make modeling difficult. All the sample data are obtained on equivalent capacitance conversion equipment, which greatly shortens the modeling time. The conversion from frequency to humidity is based on piecewise polynomial fitting. The working current of the transmitter in the prototype is 0.14 mA. The frequency resolution reaches to 0.1 Hz and the humidity measurement mean value error is less than 1.5%RH when the prototype is calibrated by saturated salt solution. The prototype connects to the membrane gas separation assembly based on polydimethylsiloxane membrane. The monitoring of membrane condition by humidity measurement method is experimentally verified in the pressure ranges from 1 MPa to 20 MPa.

INDEX TERMS Humidity measurement, membrane condition monitoring, piecewise fitting, LC-type oscillation, underwater spectrometer.

I. INTRODUCTION

Membrane-based separation technologies are important means to analyze the chemical and isotopic composition of the dissolved gases and understand the dynamic process of marine environment. It is widely applied in different fields, such as transformer insulation, environmental monitoring and search for natural gas reservoirs. For underwater spectrometers the membrane assembly is an indispensable part [1], [2]. A typical scheme of underwater spectrometer with membrane assembly is shown in Fig. 1. Seawater flows from the inlet through the pump, flows through the membrane, and is discharged through the outlet. The separated gases enter the analytical chamber. When the spectrometer operates, the measurement results should be converted in accordance with Fick's law to reveal the characteristics of dissolved gases in seawater. The membrane working condition and effectiveness play an important role during conversion.

Due to the deposition of suspended or dissolved substances on its external surfaces, at its pore openings, or within its pores, the performance of a membrane deteriorates. The data obtained under abnormal condition of membrane often lead to unexplained. In the worst case, seawater enters the spectrometer through the broken membrane, causing huge

The associate editor coordinating the review of this manuscript and approving it for publication was Haiyong Zheng.

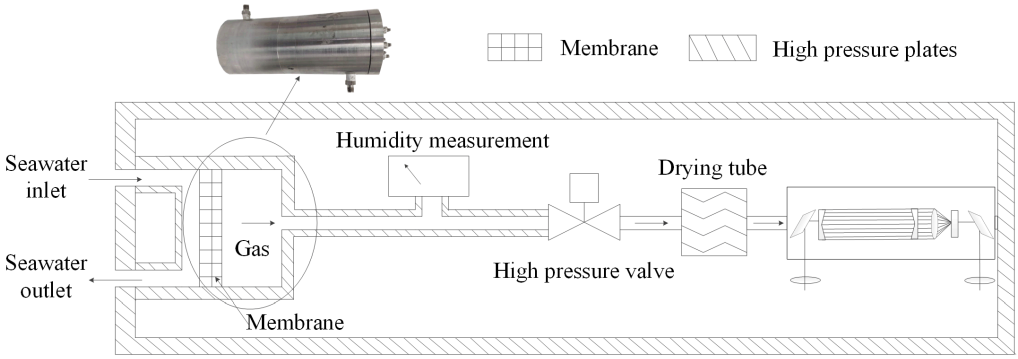

FIGURE 1. Structure of underwater spectrometer with membrane assembly.

losses. Therefore, the membrane condition monitoring is urgently necessary. Many methods had been presented to monitor the condition of membrane, such as impedance analysis [3], Raman spectroscopy [4], and vibrational spectroscopic imaging [5]. However the membrane in the underwater spectrometer is closed by thick metal plates which prevent the application of optical methods. The limited space makes it impossible to install any humidity sensor inside the membrane assembly. Flux is an important parameter used to describe the condition of membrane. The humidity of membrane separation gas depends on the water vapor flux. The condition monitoring of membrane may be realized by measuring gas humidity.

For limited inner space, the contactless and nondestructive methods for humidity measurement are convenient. The humidity sensing principle is always based on the changes of the capacitance. The samples, such as wood chips [6], corn ear [7], [8] were placed into parallel-plate capacitance and the water vapor inside samples changed the permittivity of the dielectric. The moisture content was measured by calculating the amplitude attenuation and phase shift of microwave signal. However, the membrane separation gas pipe is made of pressure resistant materials, such as stainless steel (SS) or Teflon, and its permittivity is almost independent of gas humidity. It seems to be a simple and direct method to measure the humidity of membrane separation gas by installing sensors or transmitters on the pipe, as shown in Figure 1. Zhou *et al.* [9] designed a test cell at the intersection of two gas pipe to measure the dynamic characteristic of micro-humidity sensor. The cell provided a closed space to ensure that the humidity measurement was carried out after the gas reaches equilibrium. A thin layer of moisture absorbing phosphorus pentoxide covered on the inner surface of glass tube to separate the moisture in the mineral oil of transformer. At the same time, the gas decomposition on the layer generated current, which was used to calculate the gas humidity [10]. The complex gas diffusion path makes the calibration of underwater spectrometer more difficult. The cell or the path for humidity measurement shall be designed carefully to avoid interference with the target gas of underwater spectrometers.

The safety requirement is another challenge for humidity measurement of the membrane separation gas. The working depth of the underwater spectrometer is required to reach several thousand meters. In order to prevent seawater from entering the inside when the membrane is damaged, the housing of the humidity measurement unit needs a pressure resistant design. Compared with the wired measurement method, the wireless measurement method does not need cable connection, and meets the safety requirements better. A wireless humidity measurement system is usually divided into two parts: sensor unit and readout unit. Only the sensor unit is exposed to the monitored environment [11], [12], [13]. Xie *et al.* [11] presented a paper-based *LC* wireless humidity sensor to monitor the humidity inside of sealed medicine. It was shown that the relative position between the two coils seriously affected the read resonance frequency. A humidity sensing device was developed in standard CMOS process technology. Power and data exchanged between external circuit and the device were implemented by a pair of inductive coils [12]. A low-cost digital hygrometer with passive wireless tag was developed to measure trace moisture. Experiments conducted that the reliable transmission distance at 2.4 GHz reached to 12 m when large metallic and insulting objects were placed between the tag and the read unit [13]. In these literatures, RF (radio frequency) signals are used for transmission between the sensor and the readout. The medium between them is non-metallic or non-enclosed metal plates. For a closed metallic housing, communication by RF signal is still challenging. Many studies have discussed the condition monitoring of objects with metal wall [14], [15], [16]. However, these methods were unsuitable for humidity measurement because the characteristics of permanent magnets were unaffected by ambient humidity. A feasible method is to reduce the frequency of transmission signal to pass through closed metal shell. The lower the signal frequency is, the stronger the ability to pass through the metal medium is. But the performance of capacitive humidity sensor depends heavily on the working frequency. Rahman *et al.* [17] posted the capacitance changes of humidity sensor when the humidity increased from 45%RH to 95%RH. The change of capacitance at 1 kHz was nearly 40 times of that at 10 kHz.

Islam and Rahman [18] presented the influence of the signal frequency on the response characteristics of a ceramic thin-film humidity sensor. When the sensor worked at 5 kHz, it had high resolution, which was 72 times that of 1MHz. But the nonlinearity and the hysteresis of the sensor were more serious at 5 kHz than at 1 MHz. The weakness of low frequency characteristic for humidity sensor should be avoided during measurement.

A new wireless humidity measurement method for deep-sea membrane condition monitoring by using low-frequency signal is presented. A simulation model is set up by using COMSOL Multiphysics software to investigate the efficiency of power transmission for different materials and different frequency. The influence of multiple parameters such as the thickness of metal plate on the transmission frequency was presented. A valve-like wireless humidity measurement prototype is designed. The modeling of the prototype is based on equivalent capacitance conversion equipment, which greatly shortens the modeling time. The frequency resolution is 0.1 Hz when the working frequency is about 10 kHz. The mean value error of humidity is less than 1.5%RH by using saturated salt solutions calibration. The monitoring of membrane condition by humidity measurement method is experimentally verified when the pressure changes from 1 MPa to 20 MPa.

The rest of this article is organized as follows. Section II introduces the proposed humidity measurement method. Section III discusses the design of wireless humidity measurement and its transmission characteristic analysis. Section IV constructs a prototype and equivalent capacitance conversion equipment. Section V presents the experimental results to demonstrate the performance of humidity measurement. Section VI provides the conclusions.

II. MEASUREMENT THEORY AND METHOD

A. RELATION BETWEEN GAS FLUX AND RH

PDMS (polydimethylsiloxane) is a nonporous membrane through which gas permeation occurs via the solution-diffusion mechanism. The permeation flux of water vapor under steady-state can be expressed as [19]:

$$J_w = Q(p_{sw} - p_{mv})/L, \tag{1}$$

where J_w is the permeation flux, Q is the permeability, L is the thickness of membrane, p_{sw} is equivalent partial pressure of water vapor in the seawater, p_{mv} is partial pressure of water vapor on the permeate side. Assume the statured pressure on the permeate side for the steady state is p_{sa}, the (1) can be rewritten:

$$\begin{aligned} J_w &= Qp_{sw}/L - Qp_{sa}/L \times p_m/p_{sa} \\ &= Qp_{sw}/L - Qp_{sa}/L \times RH. \end{aligned} \tag{2}$$

where, RH is the relative humidity on the membrane side.

If the temperature remains unchanged and the gas pipe is vacuumed for each measurement on the membrane side, p_{sa} can be regarded as a constant. The parameter p_{sw} is approximately invariant for seawater [20]. The derivative of J_w with respect to RH is

$$dJ_w = -Qp_{sa}/L \times dRH. \tag{3}$$

The total flux of PDMS membrane for underwater spectrometer is small, and the flux of water vapor is less. So, the RH of membrane separation gas keeps nearly unchanged for steady state. In this paper the membrane states are divided into four types: normal, fouling, partial fouling, and damage. The humidity of membrane separation gas in the fouling or damage state is obviously different from that in the normal state. The three states, normal, fouling, and damage, can be monitored by measuring the humidity of membrane separation gas when the spectrometer works. Partial fouling state is difficult to distinguish because the variation of humidity is so small in steady condition. A water vapor accumulation in constant time period is adopted to increase the variation of humidity. The gas pipe and part of the humidity measurement prototype compose a small and closed cell to estimate the partial fouling state.

B. HUMIDITY MEASUREMENT METHOD AND MODELING

The wireless humidity measurement is composed of a transmitter unit and a receiver unit. The transmitter is required to transform the humidity into the signal frequency by adopting an *LC*-type oscillating circuit. The low-frequency sinusoidal signal generated by the oscillator passes through the metallic plate and is received on the other side of the plate. The frequency of oscillator f_{os} is expressed as

$$f_{os} = \frac{1}{2\pi\sqrt{L_T C_h}}, \tag{4}$$

where C_h is the capacitor of humidity sensor, and L_T is the inductor in the *LC* oscillator.

However, the metal medium may cause a change in the signal frequency during transmission. The frequency of received signal is expressed as

$$f = f_{os} + f_{tr}, \tag{5}$$

where f_{tr} denotes the frequency offset caused by signal transmission. It is related to the thickness, the material, the location of plate and ambient temperature. A non-linear relationship exists between humidity and signal frequency. The piecewise fitting method is presented to approximate the relationship.

The modeling of humidity measurement is time-cost process because it takes a long time for humidity environment to reach stable state. The model may be required to build again for some parameters change.

Equivalent capacitance conversion is designed to shorten the time for modeling. In Figure 2, the two capacitances humidity sensors C_h and C_r are with the same type and work in same humidity environment. The C_r is dealt as the equivalent capacitance of C_h under different stimulus signals provided by LCR meter. Data sampling for modeling start when the frequency of received signal and the capacitance of reference sensor change synchronously. Waiting for the

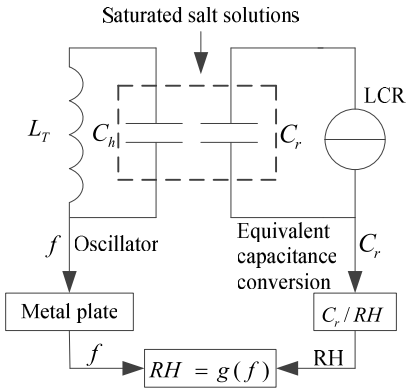

FIGURE 2. Modeling based on equivalent capacitance conversion.

humidity to stabilize for a long time is unnecessary. The conversion from capacitance to humidity is implemented according to the datasheet of humidity sensor [21]. The model of humidity measurement can be set up based on curve fitting.

C. SELECTION OF MATERIALS AND OSCILLATING FREQUENCY

The transmitter is surrounded by thick metal plates to resist high hydrostatic pressure of deep seawater. The selection of appropriate metal materials helps in signal transmission and meets the safety requirements. Two metal pressure materials, SS and aluminum (AL) are studied. A simulation model is set up for the selection of materials and oscillating frequency on COMSOL Multiphysics software. The model consists of a transmitting network, a receiving network, and a metal plate between two networks. The transmitting network consists of a uniform and multiturn coil and a capacitor. The receiving network has the same structure. The parameters of the model and the material properties of plates are shown in Table 1. The power of transmitting network is supplied by a current source. The oscillating frequency changes from 10 kHz to 100 kHz at 10 kHz intervals. The maximum efficiency of power transmission for the selected frequency is expressed as

$$\eta_{\max} = P_{r\max} / P_{t\max}, \tag{6}$$

where $P_{r\max}$ is the maximum of receiver power, and $P_{t\max}$ is the maximum of transmitter power.

From the curves of Figure 3(a), the maximum efficiency of power transmission reduces when the oscillating frequency in the SS material increases. The maximum efficiency approaches 30% when the frequency is 10 kHz. If the oscillating frequency rises up to 80 kHz, then the maximum efficiency reduces to 2%. The efficiency of power transmission in the AL material keeps at a low level in all selected frequencies.

The resonant frequencies of transmitting network and receiving network are set to 10 kHz. The frequency of source signal sweeps around the resonant frequency. The power curves of transmitting network and receiving network are

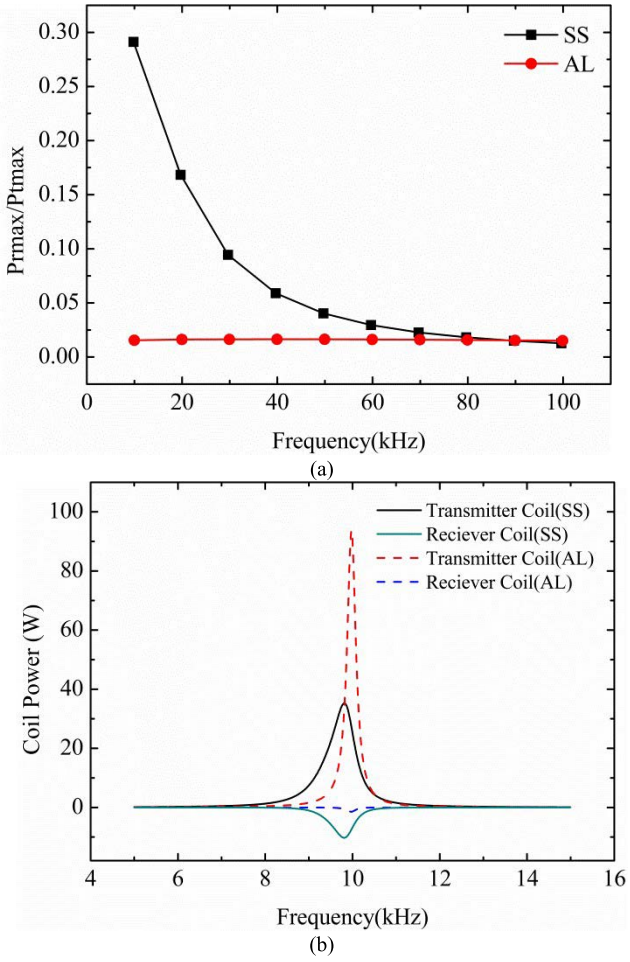

FIGURE 3. Simulation for power transmission. (a) maximum efficiency in different frequencies (b) efficiency curve at 10 kHz.

shown in Figure 3(b). For the SS material plate, the power of transmitting network reaches a maximum of about 40 W when the frequency of source signal is the same as the resonant frequency of transmitting network. If the frequency of source signal offsets 0.5 kHz from the resonant frequency, then the power reduces to 32 W. The transmission still occurs successfully when the frequency of source signal deviates from the resonant frequency. For the AL material, the bandwidth of transmitting network is narrow. The parameters of receiving network should be adjusted carefully to receive the signal. In the following chapters, the resonant frequency is designed around 10 kHz, and the shell of the transmitter is composed of SS material.

III. CIRCUIT DESIGN AND TRANSMISSION CHARACTERISTIC ANALYSIS

A. OSCILLATION CIRCUIT AND THE TRANSMITTER

As shown in Figure 4, the oscillating circuit comprises two transistors T_1 and T_2 in cascade. The frequency of oscillator is set by the choke inductor L_1 and the humidity sensor C_1 in parallel. No other capacitor is connected to the oscillation

TABLE 1. Parameter setting for the simulation.

Key parameters		Set value
Geometric structure	Outer Diameter (mm)	35
	Inner Diameter (mm)	25
	Height (mm)	5
	Number of windings	60
	Cross sectional area (mm^2)	1
Material properties	Relative Permeability (SS)	1
	Conductivity (SS, S/m)	1.137×10^6
	Relative Permeability (AL)	1
	Conductivity (AL, S/m)	3.774×10^7

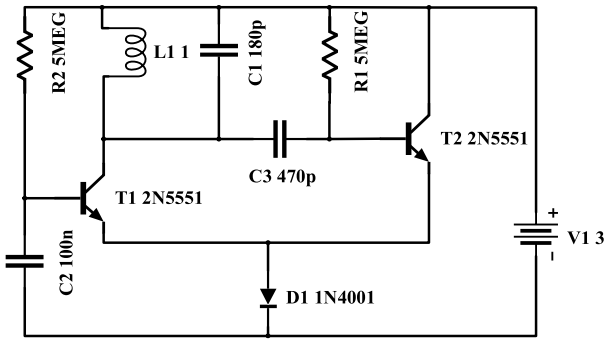

FIGURE 4. Design of oscillation circuit.

circuit to improve the resolution of humidity measurement. The amplitude of the oscillating waveform can be adjusted through the resistor R_2 and the diode D_1. The capacitance of the humidity sensor C_1 HS1101LF is around 180 pF when operating at 10 kHz and 55%RH. In the transmission characteristic analysis, the transmitter comprises the oscillator and a voltage follower. It is supplied with a button battery CR1220 at 3 V. The current is about 0.14 mA when the transmitter operates. A low noise and zero-drift operational amplifier OPA2182 is used to implement the voltage follower. The input impedance of OPA2182 in common-mode is 60 TΩ and 2.3 pF. The selection of operational amplifier with small input capacitance is helpful to reduce the interference introduced by measurement instrument input ends. However, the voltage follower in the prototype is useless and omitted from the transmitter unit.

B. FREQUENCY MEASUREMENT AND RECEIVER

The receiver consists of three circuits.

1) *LC-type network:* It is composed of a radial choke inductor and a capacitor that are connected in parallel. The inductor of the receiver is the same with that of the transmitter. The capacitor can be a constant value or provided by the humidity sensor HS1101LF.
2) *Voltage follower:* As described in transmitter part, the design of voltage follower in the receiver is the same. The function of voltage follower is to reduce the capacitance interference with *LC*-type network causing by multimeter input ends.
3) *Variable gain amplifier:* The gain of amplifier is regulated by a slide rheostat to match the different thicknesses of metal plate. For weak signal, the gain is 16, otherwise it is 1.

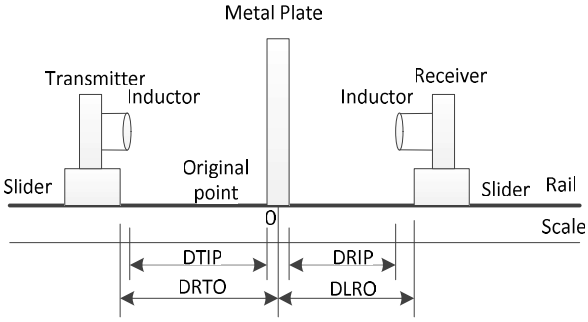

DTIP: The distance from the top of transmitter inductor to the plate
DRIP: The distance from the top of receiver inductor to the plate
DRTO: The distance from the right edge of transmitter to the original point
DLRO: The distance from the left edge of receiver to the original point

FIGURE 5. Definition of different movement distances.

C. FREQUENCY TRANSMISSION CHARACTERISTIC ANALYSIS

A test system is setup to understand the characteristic of low-frequency signal on SS material plates. The test system is composed of scale, rail, sliders, bases, and accessories. The metal plate for the test is fixed on two bases. The rail is placed under the plate vertically. Two sliders located on either side of the metal plate can move smoothly on the rail. The transmitter and the receiver are installed on the slider through the accessories. The scale parallel to the rail is pasted on the table. The supply power of transmitting side is isolated from that of the receiver side. Two six and a half digit multimeters, DMM6500 (Tektronix, USA) and 34461A (Keysight, USA), are used to read the frequency and the amplitude of signals from the transmitter and receiver separately. For clarity, the abbreviations of four movement distances, DTIP, DRIP, DRTO, and DLRO, are defined, as shown in Figure 5. The thickness of SS (SUS304) plates is 2, 4, 6, 8, and 10 mm.

1) EDDY CURRENT EFFECT

Plates of two thicknesses, 4 and 6 mm, are selected to test the influence of eddy current on low-frequency signal transmission. The test is completed in a lab room. The humidity and the temperature of environment are about 70%RH and 30°C, respectively. The receiver is fixed on the rail. DLRO is 4 cm, and DRTO can be adjusted manually. The frequency measurement curves of the receiver are shown in Figure 6. Each curve has similar characteristics and can be divided into three zones.

Sensitive zone: It is shown as ① in the two curves. When DTIP is less than 2 mm, the frequency of the received signal is unstable. Slight variation in distance can lead to a large offset of frequency. The most serious case is that damped oscillation

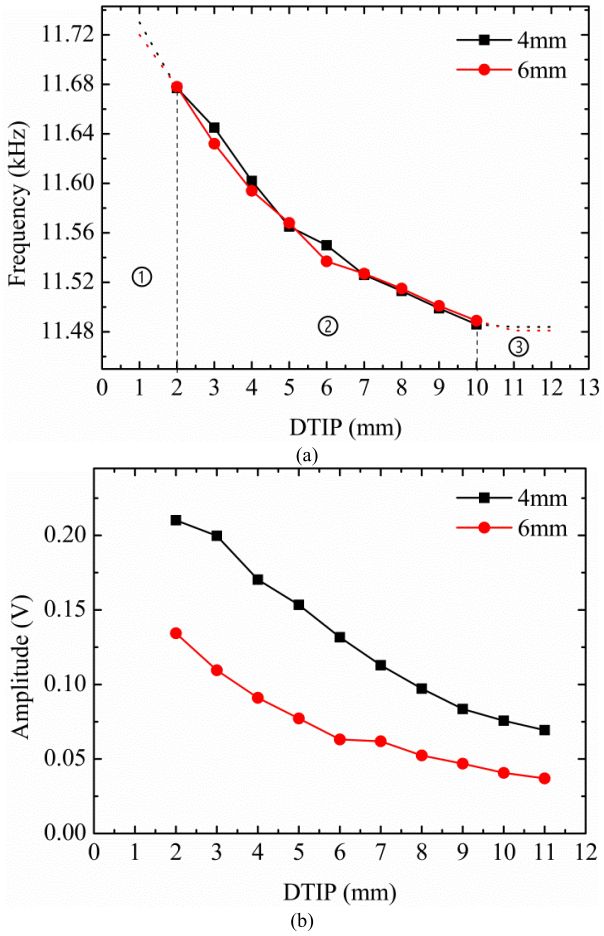

FIGURE 6. Influence of eddying effect for signal passing. (a) frequency (b) amplitude.

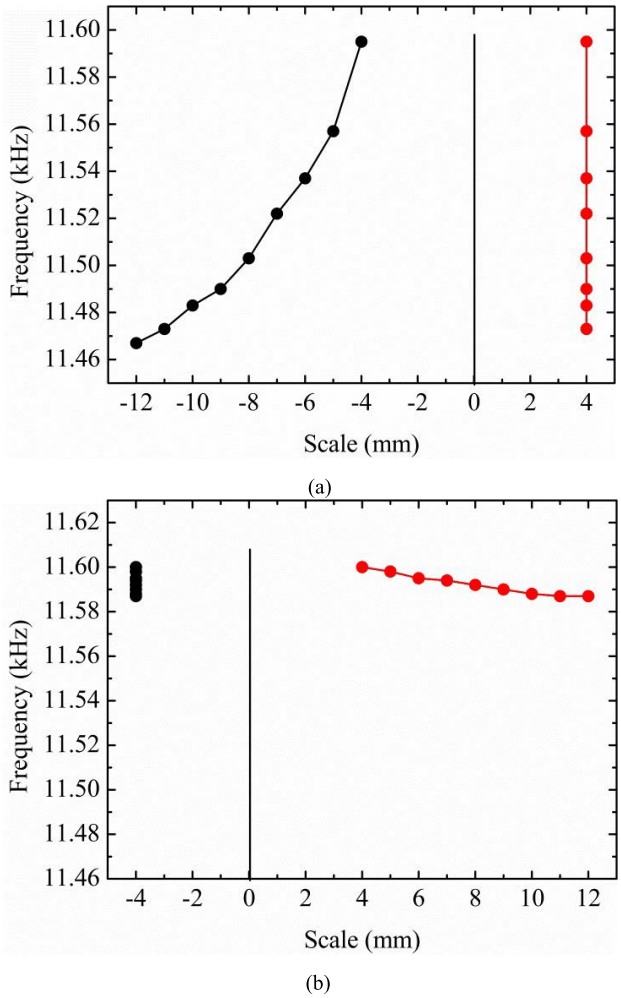

FIGURE 7. Frequency response of transmitter and receiver movements. (a) transmitter moves, receiver stays (b) transmitter stays, receiver moves.

may occur. Therefore, the transmitter should be prevented from operating in the sensitive zone. A safety distance must be kept when fixing the transmitter.

Stable zone: It is shown as ② in the two curves. The frequency of the signal is stable if the transmitter stays on the rail. The thickness of metal plate exhibits weak influence on the frequency. However, the amplitude of the received signal reduces sharply when the plate thickness increases, as shown in Figure 6(b). Computing the humidity by measuring the frequency rather than the amplitude of the received signal is reasonable.

Invalid zone: It is shown as ③ in the two curves. The area of plate is limited, which is 100 mm high and 250 mm long. The magnetic field may bypass the metal plates. Thus, the frequency of the received signal is unaffected by the eddy current effect and remains at a fixed value. The reading of frequency measurement cannot reveal the status of humidity sensor.

2) DIFFERENT PERFORMANCE OF TRANSMITTER AND RECEIVER MOVEMENTS

Transmitter movement and receiver movement generate different results. In Figure 7(a), DLRO is 4 mm. The transmitter moves opposite to the receiver. The frequency of the received signal decreases when the distance between the transmitter and the receiver increases. In Figure 7(b), the receiver moves opposite to the transmitter, and DRTO is 4 mm. However, the frequency of the received signal declines slightly. The frequency of the received signal is sensitive to the movement of transmitter. For example, when the transmitter is 4mm away from the metal plate, every 0.1 mm distance deviation will cause a frequency offset of 3Hz, which equals to 2%RH humidity measurement error under low RH condition. Regardless of how the transmitter or the receiver moves or stays, the operating frequency of transmitter is the same as that of receiver if the whole system operates in the stable zone.

3) EFFECT OF METAL PLATE THICKNESS

For the SS material plate, DTIP is greater than 2 mm, which makes the transmitter work in the stable zone. The maximum thickness of SS plate in this paper is 10 mm. The frequency curve is shown in Figure 8. The zero thickness denotes that no plate exists between the transmitter and receiver. The frequency increases with the increase in plate thickness. However, the frequency for the 10 mm-thick plate is less than

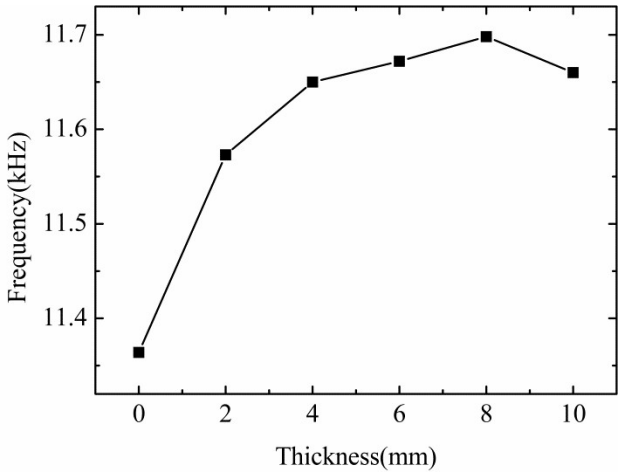

FIGURE 8. Influence of plate thickness on measurement.

FIGURE 9. Prototype of humidity measurement. (a) installation of transmitter (b) installation of receiver.

that of the 8 mm–thick plate. When the 10 mm-thick plate is placed, the receiver may enter the sensitive zone.

When the thickness of SS plate is increased from 4mm to 8mm, the frequency deviation is about 50Hz. The above results show that the frequency of receiver signal depends on many factors. If one of these factors changes, the whole measurement system needs to be modeled again. In this paper, we construct a set of equivalent capacitance conversion equipment to reduce the time for modeling.

IV. MEASUREMENT PROTOTYPE SETUP AND TEST

A. PROTOTYPE SETUP

A prototype with a high-pressure valve chamber is established. The chamber composes two parts: base and cap. They are connected by six bolts and sealed with an O-ring seal. The transmitter is mounted on the base of chamber, as shown in Figure 9(a). The receiver is fastened on the cap. The outer shape of the valve chamber is shown in Figure 9(b). The inductors of the transmitter and the receiver are aligned in the center of the cap. The valve chamber is made of SS material. The cap thickness is 5 mm.

There is a gas path in the base to connect with pipe of membrane separation gas. The humidity sensor whose shell has been removed is placed at the end of gas path. A cylindrical recess is designed to accommodate the humidity sensor. The

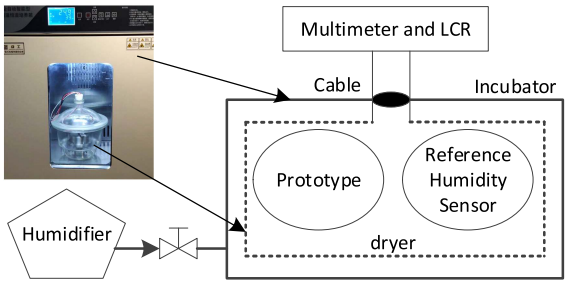

FIGURE 10. Equivalent capacitance conversion equipment.

humidity sensor is sealed in the recess, and only two pins are connected to the oscillation circuit. The gas path in the base and the pipe of membrane separation gas form the cell for partial fouling state monitoring.

In the transmitter, the humidity sensor is placed on the back of the printed circuit board (PCB) and the other parts on the top. The PCB board of the receiver is supported by three of the six bolts connecting the base and the cap. The distance from the top of the receiver inductor to the cap can be adjusted by turning the nuts on the bolts.

B. EQUIVALENT CAPACITANCE CONVERSION EQUIPMENT

As shown in Figure 10, the equivalent capacitance conversion equipment is composed of an incubator, a humidifier, and accessories. The multimeter 34461A is used to read the frequency of output signal. An LCR instrument TH2832 (Tonghui, China) is used to record the capacitance of the reference humidity sensor. The range of RH regulation is from 20% to 90% for the incubator. The sweeping frequency and the amplitude of test voltage set for the LCR meter agree with the test condition of humidity sensor characteristic curve. For the humidity sensor HS1101LF, the sweeping frequency is 10 kHz, and the amplitude of test voltage is 1 V The main function of equivalent capacitance conversion equipment is to generate sufficient sample data for prototype modeling and calibration.

The accuracy of temperature control for the incubator is 0.1°C. A dryer with saturated salt solution is added to the incubator to provide stable humidity test conditions. Moreover, the humidity for each saturated salt solution is as a reference to estimate the humidity measurement error. The distance from the humidity sensor to the surface of salt solution is about 3 mm. The dryer is sealed with a rubber plug. The cables of the prototype pass through the rubber plug and are connected to the power supplier and instruments.

C. VERIFICATION WITH THE MEMBRANE GAS SEPARATION ASSEMBLY

The prototype is linked into the membrane separation assembly to evaluate its performance in membrane gas separation. The inlet of the prototype is connected to the gas outlet of the membrane separation assembly by a control valve S1 (SS-2MG-MH, Swagelok, USA). The outlet of the prototype

and a flow controller D08-1F (Sevenstar, China) are joined together by the other valve S2. A vacuum pump N84 (KNF, Germany) is installed at the outlet of the flow controller. The pressure of membrane separation assembly is regulated manually. The pressure value is displayed by a pressure meter Datum 2000 (Setra, USA). In each experiment, the gas in the cell of the prototype is excluded until the flow is less than 0.02 mL/min and the frequency of the prototype remains unchanged. The outlet of the prototype is closed, and the inlet is opened. The membrane separation gas enters the cell of the prototype and the humidity measurement starts. The membrane adopted in the experiment is PDMS, and its effective section area is about 23.6 cm^2.

V. RESULTS AND DISCUSSION

A. DATA SAMPLING AND FITTING

1) SAMPLING DATA

If the membrane is damaged, the humidity of gas will rise quickly and reach to a saturated condition. On the contrary, the humidity is very low if the membrane is completely fouling. The two states are easy to monitor. Therefore, the arrangement of sampling is mainly for normal and partial fouling states of membrane separation gas. The range of humidity is set from 30%RH to 80%RH. There are five salt saturated solutions for humidity measurement, Magnesium Chloride (MC), Potassium Carbonate (PC), Sodium Bromide (SB), Potassium Iodide (PI), and Sodium Chloride (SC). According to the recommendations of OIML (International Organization for legal metrology), the humidity mean values of the five salt saturated solutions at 25°C are 32.8%RH, 43.2%RH and 57.6%RH, 68.9%RH and 75.3%RH respectively.

Considering that the temperature fluctuation range of deep-sea water is about 2°C, data sampling is conducted under three temperature conditions: 27°C, 25°C and 23°C. The sampling time of each solution at each temperature is more than 6 hours, and the data are recorded every 10 minutes. To test the performance of modeling based on equivalent capacitance conversion, the data in an hour after the sample begins (named as ''1 h'') and the data in an hour before the sample ends (named as ''6 h'') are selected.

2) DATA FITTING

The piecewise polynomial curve fitting is adopted to convert the frequency to humidity. The fitting curves of data in 25°C are shown in Figure 11. The curve is divided into two parts and each part is represented by a polynomial equation. If the frequency is less than 11.9250 kHz for 6h data, the equation is

$$\%RH = -184.556f^3 + 6491.811f^2 - 76167.722f + 298141.308$$

else the equation is

$$\%RH = -22858.035f^2 + 544459.808f - 3242103.569. \quad (7)$$

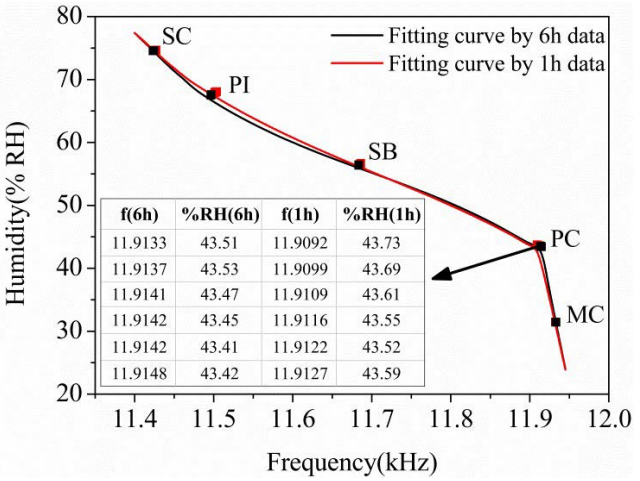

FIGURE 11. Fitting curves for 1h data and 6h data.

TABLE 2. Frequency measurement for saturated salt solutions of 6h.

T(°C)	PI(kHz)		SB(kHz)		MC(kHz)	
	Max	Min	Max	Min	Max	Min
27	11.4826	11.4830	11.6664	11.6650	11.9251	11.9247
25	11.4969	11.4963	11.6837	11.6834	11.9326	11.9329
23	11.5136	11.5126	11.7053	11.7050	11.9471	11.9475

The stability of 6h data is better than that of 1h data which can be deduced from the data distribution of PC solution in Figure 11. However, the two fitting curves mostly overlap. The maximum deviation of the two fitting curves is caused by PI saturated salt solution whose output frequency declines with the time rather than fluctuates at equilibrium. This phenomenon is related to the characteristics of the sensor in the high humidity environment, because in the incubator without saturated solution, this phenomenon also has been observed.

B. HUMIDITY MEASUREMENT ACCURACY

1) MEASUREMENT SENSITIVITY

The results of frequency measurement in three representative salt solutions, MC (low RH), SB (moderate RH), PI (high RH), are displayed in Table 2. Four significant digits are reserved in each datum limited by the function of the multimeter 34461A. At the set temperatures, the frequency resolution of all three solutions reaches 0.1 Hz. For most of 6h data, except the SB solution in 27°C, the frequency variation is less than 1Hz. The data distribution indicates that the humidity measurement system has high stability at low frequency.

The low frequency characteristics of humidity sensors show great differences with the change of humidity. The relation between the change of frequency and the change of humidity in the set temperature are shown in Table 3. The sensitivity of humidity measurement is expressed as

$$S = \Delta f / \Delta H. \quad (8)$$

TABLE 3. Humidity and frequency changes at different temperatures.

	27°C		25°C		23°C	
	ΔH (%RH)	Δf (Hz)	ΔH (%RH)	Δf (Hz)	ΔH (%RH)	Δf (Hz)
MC-PC	11.83	18.50	12.04	19.00	11.98	23.10
PC-SB	13.56	240.60	12.93	230.50	12.71	219.00
SB-PI	10.90	183.00	11.14	186.90	11.16	192.00
PI-SC	6.67	83.00	7.04	72.60	7.14	82.00

The sensitivity fluctuates greatly under different humidity levels. The maximum of S is 17.8 Hz/%RH when the humidity increases from 43.2%RH to 57.6%RH. The minimum of S is 1.6 Hz/%RH when the humidity increases from 32.8%RH to 43.2%RH. Refer to (8), when the frequency resolution is 0.1Hz, the resolution is 0.06%RH at low humidity and 0.006%RH at medium humidity. Under three different temperature conditions, the humidity sensitivity is similar, which indicates that small temperature fluctuations have little impact on the sensitivity of humidity measurement.

2) MEASUREMENT TRUENESS

OIML recommends the fluctuating range of humidity at a constant temperature for each saturated salt solution. The trueness of humidity measurement in an hour is described by the mean value error

$$\delta_{nh} = \overline{H}_{OIML} - \overline{H}_{nh}. \tag{9}$$

where n is 1 or 6.

The mean values and the error are shown in Figure 12. The mean value error is less than 1.5%RH for all the saturated salt solution which indicates the humidity measurement with equivalent conversion equipment owns high trueness. It also can be inferred that there is a systematic error in the humidity measurement because most of the mean value errors are greater than zero. This may be due to the lack of stirring the salt solution. There is not enough space in the dryer to install stirring equipment.

The maximum of mean value error, 1.37%RH for 6h data and 1.36%RH for 1h data, occurs in MC solution. The minimum of mean value error, −0.26%RH for 6h data and −0.42%RH for1h data, happens at PC solution. The distribution of mean value error maybe relates to the features of salt solutions, not have much to do with the low frequency characteristics of humidity sensor. The frequency fluctuation in MC solution is less than that of PC solution by comparing the data in Table 2 and Figure 11.

The mean value error of 1h data is similar to that of 6h data, and even less for some solutions. Therefore, longer solution stabilization time does not help much to improve the measurement trueness. This result verifies that it is effective to short the modeling time through equivalent capacitance conversion.

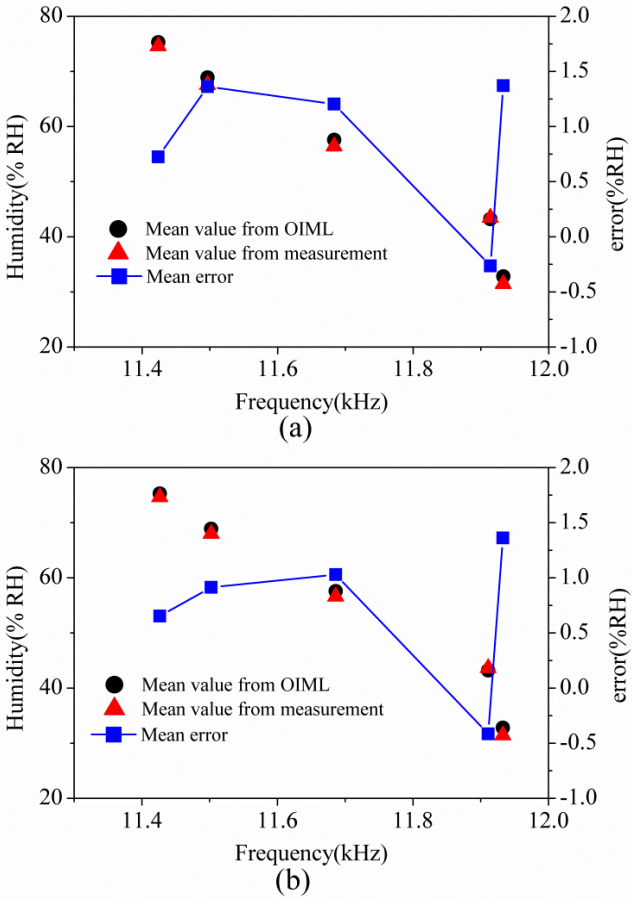

FIGURE 12. Humidity measurement mean value error, (a) 6h data (b) 1h data.

3) MEASUREMENT PRECISION

The precision of humidity measurement is evaluated by multiple parameters of polynomial fitting error. The parameters consist of error maximum (EMAX), root mean square value of error (RMSE) and coefficient of determination (R^2). The RMSE is defined as

$$RMSE = \sqrt{\frac{1}{N}\sum_{i=1}^{N}(g(f_i) - RH_i)^2}. \tag{10}$$

where f_i is the ith frequency of humidity measurement data, g denotes the fitting function, RH_i is the relative humidity according to f_i, N is the total amount of data.

The results are shown in Table 4. The values of R^2 for all the fitting curves approach to 1, which discloses that the data have been fitted well. Though all the RMSE for 6h data is better than that of 1h data, it is still on the same order of magnitude. The EMAX 0.72%RH at 27°C and 0.62%RH at 23°C are both derived from 1h data of MC solution, which indicates that MC solution needs long time to reach stability.

The measurement precision in the Part II seems worse than that in the Part I, because the number of fitting data in the Part II is only half of that in the Part I.

TABLE 4. Polynomial fitting error.

T(°C)	Data	Fitting equations					
		Part I			Part II		
		R^2	RMSE (%RH)	EMAX (%RH)	R^2	RMSE (%RH)	EMAX (%RH)
27	6h	0.99	0.03	0.06	0.99	0.14	0.28
	1h	0.99	0.10	0.22	0.99	0.28	0.72
25	6h	0.99	0.03	0.14	0.99	0.12	0.34
	1h	0.99	0.08	0.18	0.99	0.14	0.26
23	6h	0.99	0.04	0.09	0.99	0.09	0.16
	1h	0.99	0.09	0.19	0.98	0.34	0.62

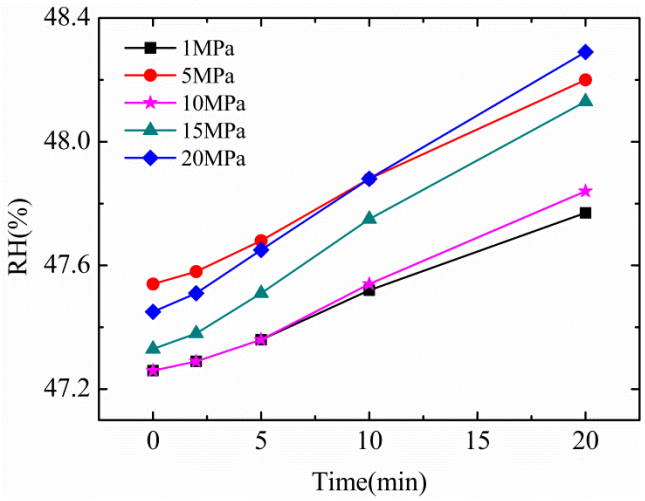

FIGURE 13. Humidity measurement of prototype under different pressures.

C. HUMIDITY MEASUREMENT WITH MEMBRANE GAS SEPARATION

The The water used in the experiment is obtained from the laboratory. The water pressure of membrane separation assembly is set to 1, 5, 10, 15, and 20 MPa. The humidity starts to be recorded when the gas inlet of the prototype is open. The other data are sampled at 2, 5, 10, and 20 min. When the humidity measurement is completed at a set pressure, the prototype is disconnected from the membrane separation assembly. The humidity gradually returns to the initial state before the next measurement, so as to ensure that the test conditions are consistent. The results are shown in Figure 13. Before each measurement, the vacuum pump extracts the air from the prototype until the humidity of the prototype does not change. This process discloses the humidity level when the membrane is in an invalid state.

The starting point of each curve indicates the humidity value when S1 turns on and S2 turns off. The humidity of all curves increases with time. The permeability of water gas rises with the increase in pressure, which can be deduced from the slope change in the humidity curves. When the pressure increases from 1 MPa to 5 MPa, the difference in humidity corresponding to 2, 5, 10, and 20 min is 0.01%RH, 0.04%RH, 0.08%RH, and 0.15%RH, respectively. The results reflect that the influence of pressure change on humidity is relatively weak. This is because the flow of other dissolved gases increases at the same time. Sharp humidity change will not be observed unless the membrane is damaged.

When the pressure rises from 1 MPa to 20 MPa, the increase in humidity within 20 min is 0.52%RH, 0.66%RH, 0.59%RH, 0.80%RH, and 0.83%RH. The flux of membrane gas separation is about 0.06 mL/min. The change in humidity is obvious and can be distinguished. By comparing the increase of humidity in the same time interval, the condition of partially fouling can be monitored and estimated, and the influence of the nonlinearity and the hysteresis of the sensor working in low frequency on the humidity measurement are also be reduced.

VI. CONCLUSION

In this paper, a wireless humidity measurement method is proposed to monitor the membrane condition of underwater spectrometer. The main conclusions can be drawn:

1) It is verified that the membrane condition of underwater spectrometer can be monitored by humidity measurement. The three states, normal, fouling and damage, are distinguished with humidity when the spectrometer works. The partial fouling state is estimated by the humidity increase in a constant time interval.
2) The humidity measurement in low frequency with high frequency resolution and high humidity measurement trueness is realized. Calibration with saturated salt solutions, the frequency resolution is 0.1 Hz when the working frequency is about 10 kHz and the mean value error of humidity measurement is less than 1.5%RH.
3) Experiment results show that data sampling based on equivalent capacitance conversion shortens the modeling time greatly. The same frequency resolution and the same mean value error of humidity are achieved when the model of humidity measurement is established by using the 1h data and 6h data respectively.

REFERENCES

[1] M. S. Brennwald, M. Schmidt, J. Oser, and R. Kipfer, "A portable and autonomous mass spectrometric system for on-site environmental gas analysis," *Environ. Sci. Technol.*, vol. 50, no. 24, pp. 13455–13463, Dec. 2016.
[2] R. Grilli, "SUB-OCEAN: Subsea dissolved methane measurements using an embedded laser spectrometer technology," *Environ. Sci. Technol.*, vol. 52, pp. 10543–10551, Aug. 2018.
[3] S. Bannwarth, T. Trieu, C. Oberschelp, and M. Wessling, "On-line monitoring of cake layer structure during fouling on porous membranes by *in situ* electrical impedance analysis," *J. Membrane Sci.*, vol. 503, pp. 188–198, Apr. 2016.
[4] T. Virtanen, S.-P. Reinikainen, M. Kögler, M. Mänttäri, T. Viitala, and M. Kallioinen, "Real-time fouling monitoring with Raman spectroscopy," *J. Membrane Sci.*, vol. 525, pp. 312–319, Mar. 2017.
[5] C. Wei, "Evolution of membrane fouling revealed by label-free vibrational vibrational spectroscopic imaging," *Environ. Sci. Technol.*, vol. 51, no. 17, pp. 9580–9587, Aug. 2017.
[6] C. V. Kandala, R. Holser, V. Settaluri, S. Mani, and N. Puppala, "Capacitance sensing of moisture content in fuel wood chips," *IEEE Sensors J.*, vol. 16, no. 11, pp. 4509–4514, Jun. 2016.

[7] L. Fan, Z. Chai, Y. Wang, Z. Wang, P. Zhao, J. Li, Q. Zhou, X. Qin, J. Yao, S. Yan, Z. Wang, and L. Huang, "A novel handheld device for intact corn ear moisture content measurement," *IEEE Trans. Instrum. Meas.*, vol. 69, no. 11, pp. 9157–9169, Nov. 2020.

[8] J. Zhang, D. Du, Y. Bao, J. Wang, and Z. Wei, "Development of multifrequency-swept microwave sensing system for moisture measurement of sweet corn with deep neural network," *IEEE Trans. Instrum. Meas.*, vol. 69, no. 9, pp. 6446–6454, Sep. 2020.

[9] W.-H. Zhou, L.-C. Wang, and L.-B. Wang, "A method to measure the dynamic characteristics of microhumidity sensors," *IEEE Trans. Instrum. Meas.*, vol. 63, no. 12, pp. 2993–3001, Dec. 2014.

[10] M. Lyutikova, "An improved electrochemical method for moisture determination in mineral oil," *IEEE Trans. Dielectr. Electr. Insul.*, vol. 27, no. 6, pp. 2172–2178, Dec. 2020.

[11] M.-Z. Xie, L.-F. Wang, L. Dong, W.-J. Deng, and Q.-A. Huang, "Low cost paper-based LC wireless humidity sensors and distance-insensitive readout system," *IEEE Sensors J.*, vol. 19, no. 12, pp. 4717–4725, Jun. 2019.

[12] D. Cirmirakis, A. Demosthenous, N. Saeidi, and N. Donaldson, "Humidity-to-frequency sensor in CMOS technology with wireless readout," *IEEE Sensors J.*, vol. 13, no. 3, pp. 900–908, Mar. 2013.

[13] A. Siddiqui, R. Mahboob, and T. Islam, "A passive wireless tag with digital readout unit for wide range humidity measurement," *IEEE Trans. Instrum. Meas.*, vol. 66, no. 5, pp. 1013–1020, May 2017.

[14] S. Taghvaeeyan, R. Rajamani, and Z. Sun, "Non-intrusive piston position measurement system using magnetic field measurements," *IEEE Sensors J.*, vol. 13, no. 8, pp. 3106–3114, Aug. 2013.

[15] Y. Chen, O. Guba, C. F. Brooks, C. C. Roberts, B. G. Van Bloemen Waanders, and M. B. Nemer, "Remote temperature distribution sensing using permanent magnets," *IEEE Trans. Magn.*, vol. 53, no. 2, pp. 1–13, Feb. 2017.

[16] L. A. Gupta and D. Peroulis, "Wireless temperature sensor for condition monitoring of bearings operating through thick metal plates," *IEEE Sensors J.*, vol. 13, no. 6, pp. 2292–2298, Jun. 2013.

[17] M. U. Rahman, "Electrical and hysteric properties of organic compound-based humidity sensor and its dualistic interactive approach to H_2O molecules," *Mater. Today Commun.*, vol. 29, pp. 1–8, Oct. 2021.

[18] T. Islam and M. Z. U. Rahman, "Investigation of the electrical characteristics on measurement frequency of a thin-film ceramic humidity sensor," *IEEE Trans. Instrum. Meas.*, vol. 65, no. 3, pp. 694–702, Mar. 2016.

[19] X. T. Cao, H. S. Lee, and X. S. Feng, "Extraction of dissolved methane from aqueous solutions by membranes: Modelling and parametric studies," *J. Membr. Sci.*, vol. 596, Oct. 2020, Art. no. 117594.

[20] R. J. Bell, R. T. Short, F. H. Van Amerom, and R. H. Byrne, "Calibration of an *in situ* membrane inlet mass spectrometer for measurements of dissolved gases and volatile organics in seawater," *Environ. Sci. Technol.*, vol. 41, no. 23, pp. 8123–8128, 2007.

[21] *TE Connectivity. Datasheet of HS1101LF*. Accessed: Sep. 27, 2022. [Online]. Available: https://www.te.com/usa-en/product-HPP801A031.datasheet.pdf

XIAOYONG NI received the Ph.D. degree in geophysical prospecting and information technology from the China University of Geosciences, Wuhan, China, in 2009, with a focus on signal processing.

He is currently an Associate Professor with the School of Mechanical Engineering and Electronic Information, China University of Geosciences. His current research interests include the Internet of Things and applications, intelligent sensors, and embedded technology.

XUHUA CHEN received the B.E. degree in electronic information engineering from the China University of Geosciences, Wuhan, China, in 2020, where he is currently pursuing the M.Sc. degree with the School of Mechanical Engineering and Electronic Information.

His current research interests include embedded technology and software development.

YEDAN ZHANG received the B.E. degree in communication engineering from South–Central University for Nationalities, China, in 2019. She is currently pursuing the M.Sc. degree with the School of Mechanical Engineering and Electronic Information, China University of Geosciences, Wuhan.

Her research interests include database technology and software development.

WANJUN LU received the Ph.D. degree in mineral prospecting and exploration from the China University of Geosciences, Wuhan, China, in 2001.

He is currently a Professor with the College of Marine Science and Technology, China University of Geosciences. His current research interests include exploration and exploitation of marine natural gas hydrate resources.

HONGJIAN ZHANG received the M.Sc. degree in communication and information engineering from the China University of Geosciences, Wuhan, China, in 2008.

She is currently an Associate Professor at the Institute of Electronic Information, Wuhan Qingchuan University. Her current research interests include electronic circuit and embedded system development.

LIFU ZHANG is currently pursuing the Ph.D. degree with the College of Marine Science and Technology, China University of Geosciences, Wuhan.

His research interests include marine hydrate detection technology and equipment.

XIAOYU XIONG received the B.E. degree in electronic information engineering from the Wuhan Institute of Technology, China, in 2021. She is currently pursuing the M.Sc. degree with the School of Mechanical Engineering and Electronic Information, China University of Geosciences, Wuhan.

Her research interests include the IoT and software development.